

Supplemental Data

***TMEM126A*, Encoding a Mitochondrial Protein, Is Mutated**

in Autosomal-Recessive Nonsyndromic Optic Atrophy

Sylvain Hanein, Isabelle Perrault, Olivier Roche, Sylvie Gerber, Noman Khadom, Marlene Rio, Nathalie Boddaert, Marc Jean-Pierre, Nora Brahimi, Valérie Serre, Dominique Chretien, Nathalie Delphin, Lucas Fares-Taie, Sahran Lachheb, Agnès Rotig, Françoise Meire, Arnold Munnich, Jean-Louis Dufier, Josseline Kaplan, and Jean-Michel Rozet

Figure S1. Full parametric linkage analysis of Family 1 using a combination of Affymetrix GeneChip Human Mapping 10K 2.0 Arrays and microsatellite markers.

This approach points to a unique candidate region on chromosome 11 with a maximum lod-score $>+3$. Parametric LOD scores were calculated using the MERLIN¹ software program.

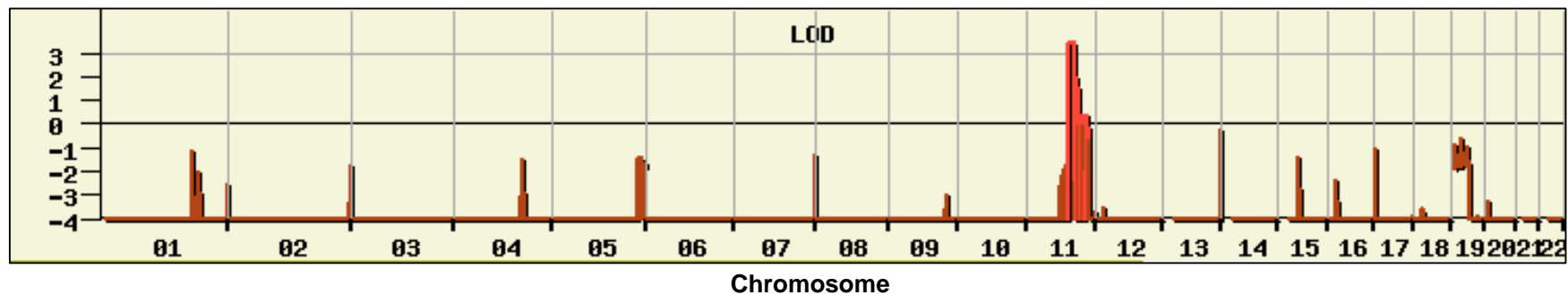


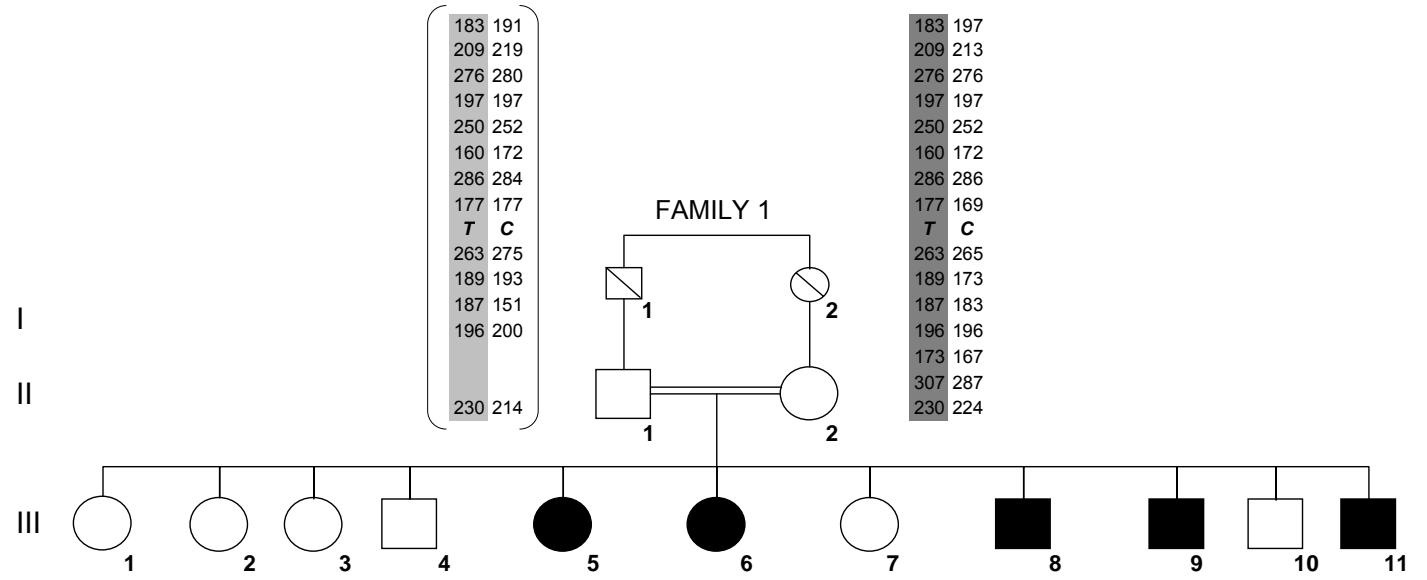
Figure S2. Localization of the *ROA2* locus and segregation of disease-causing mutations.

Pedigree structure of families 1 to 4 with haplotypes reconstruction for informative markers on chromosome 11q14.1-q21. Black circles (women) and squares (men) indicate affected members. The code numbers of all sampled individuals are given below the symbols. Chromosomal positions of SNP and microsatellite markers are indicated in Mega base pairs (Mb) according to the draft of the human genome sequence (UCSC and Ensembl databases). VNTR: variable number of tandem repeats chosen from the UCSC database (primers in the Supplementary Table). Brackets show the deduced haplotype of subject II-1. Hashes point multiallelic markers used to refine the interval indicated by the “Affimetrix 10k SNP” genome scan in individuals III-2, III-5, III-6, III-8 and III-9 (Family 1). The homozygous haplotype in which the mutated gene is most likely located in affected patients is flanked by black boxes. Arrows indicate the position of key recombination events that were used to restrict the candidate *ROA2* interval: obligatory recombination events between loci *D11S4143* and *VNTR19CA* (Family 1, patient III-9), and loci *rs2020351* and *VNTR26AT* (family 1, individual III-8), respectively, defined a 14.4 Mb interval between loci *D11S4143* and *VNTR26(AT)*. The ancestral haplotype shared by the four families is framed.

Segregation of disease-causing mutations: “C” indicates wild-type allele and “T” indicates the nonsense mutation c.163C>T, p.Arg55X. Mutations were detected after PCR of the five *TMEM126A* exons (primers in the Supplementary Table), sequencing of the purified fragments using the Big Dye chemistry version 3.1 (Applied Biosystems) and analysis using an ABI-3130 sequencer (Applied Biosystems). We have chosen to number the A of the start codon (ATG) of the cDNA sequence of the *TMEM126A* (Genbank accession numbers NM_032273) as nucleotide 1.

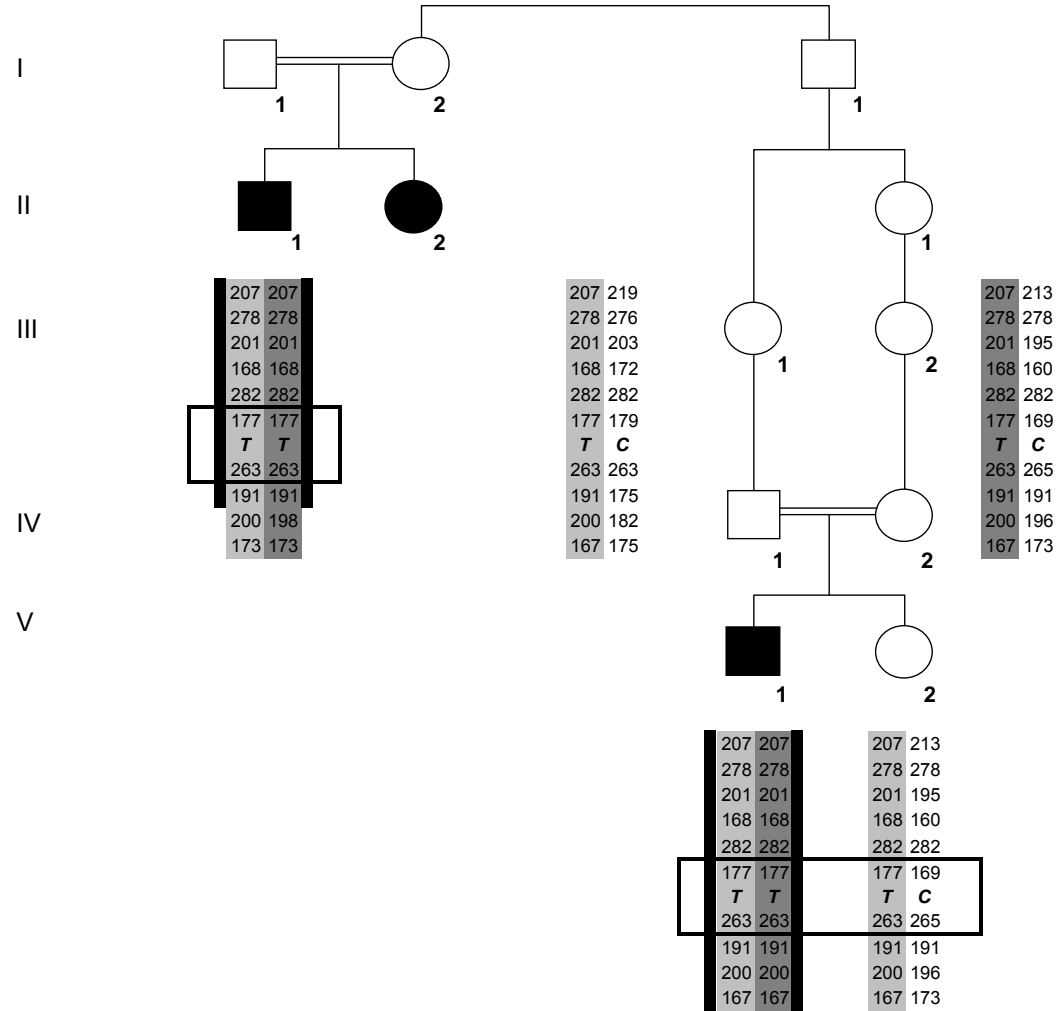
AJHG, Volume 84

MARKERS	Mb	Band
centromere		
<i>D11S918 (AFM203vq1)</i> #	78.4	11q14.1
<i>D11S4143 (AFMb055yd1)</i> #	79.03	
<i>VNTR19CA</i> #	79.28	
<i>D11S1362 (AFMa132xh9)</i> #	79.47	
<i>VNTR23TG</i> #	79.67	
<i>D11S901 (AFM063yg1)</i> #	81.52	
<i>D11S4187 (AFM311wh5)</i> #	83.23	
<i>D11S1354 (AFM338xe1)</i> #	84.35	
<i>TMEM126A - c.163C</i>	85.04	11q14.1
<i>D11S1887 (AFMa049wa5)</i> #	86.06	11q14.2
<i>D11S1780 (AFMa082wb9)</i> #	87.32	
<i>D11S4175 (AFM269yg9)</i> #	89.89	11q14.3
<i>D11S1332 (AFM281wf9)</i> #	91.74	
<i>VNTR29TA</i> #	93.41	11q21
<i>VNTR26AT</i> #	93.48	
<i>D11S4176 (AFMb354xa5)</i> #	93.71	
telomere		

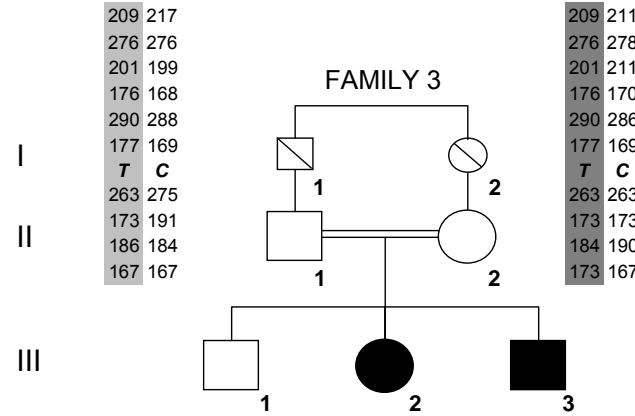


<i>D11S918 (AFM203vq1)</i> #	78.4	11q14.1	191 197	191 197	183 183	183 183	183 197	183 183	191 183	183 197
<i>D11S4143 (AFMb055yd1)</i> #	79.03		219 213	219 213	209 209	209 209	209 213	209 209	219 209	209 209
<i>VNTR19CA</i> #	79.28		280 276	280 276	276 276	276 276	276 276	276 276	276 276	276 276
<i>D11S1362 (AFMa132xh9)</i> #	79.47		197 197	197 197	197 197	197 197	197 197	197 197	197 197	197 197
<i>VNTR23TG</i> #	79.67		252 252	250 252	250 250	250 250	250 252	250 250	250 250	250 250
<i>rs1479311</i>	79.7		A A		B B	B B		B B	B B	
<i>D11S901 (AFM063yg1)</i> #	81.52		172 172	160 172	160 160	160 160	160 172	160 160	160 160	160 160
<i>rs1318423</i>	82.34		A B		B B	B B		B B	B B	
<i>D11S4187 (AFM311wh5)</i> #	83.23		284 286	286 286	286 286	286 286	286 286	286 286	286 286	286 286
<i>D11S1354 (AFM338xe1)</i> #	84.35		177 169	177 169	177 177	177 177	177 169	177 177	177 177	177 177
<i>rs1073985</i>	84.36		A B		B B	B B		B B	B B	
<i>TMEM126A - c.163C</i>	85.04	11q14.1	C C	T C	T T	T T	T C	T T	T T	T T
<i>D11S1887 (AFMa049wa5)</i> #	86.06	11q14.2	275 265	263 265	263 263	263 263	263 265	263 263	263 263	263 263
<i>rs1378879</i>	86.47		A A		B B	B B		B B	B B	
<i>D11S1780 (AFMa082wb9)</i> #	87.32		193 173	189 173	189 189	189 189	189 173	189 189	189 189	189 189
<i>rs649529</i>	87.69		B B		A A	A A		A A	A A	
<i>D11S4175 (AFM269yg9)</i> #	89.89	11q14.3	151 183	187 183	187 187	187 187	187 183	187 187	187 187	187 187
<i>rs1404527</i>	90.29		A A		B B	B B		B B	B B	
<i>D11S1332 (AFM281wf9)</i> #	91.74		200 196	196 196	196 196	196 196	196 196	196 196	196 196	196 196
<i>rs2045462</i>	92.91	11q21	A B		A A	A A		A A	A A	
<i>VNTR29TA</i> #	93.41		173 167	173 167	173 173	173 173	173 167	173 173	173 173	173 173
<i>rs2020351</i>	93.43		A B		B B	B B		B B	B B	
<i>VNTR26AT</i> #	93.48		307 287	307 287	307 307	307 307	307 287	307 287	307 307	307 307
<i>D11S4176 (AFMb354xa5)</i> #	93.71		230 224	230 224	214 230	230 230	230 224	230 224	230 230	230 230

FAMILY 2



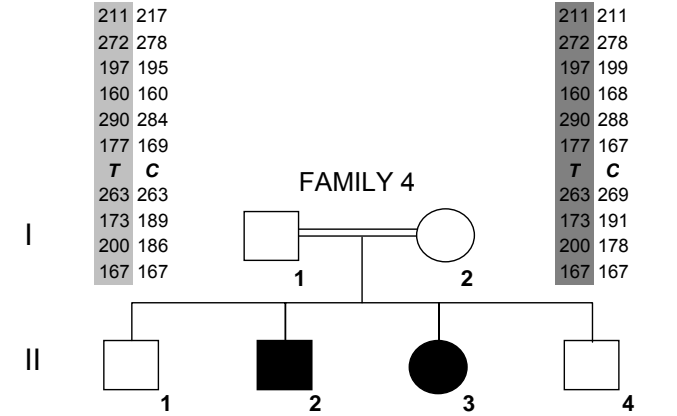
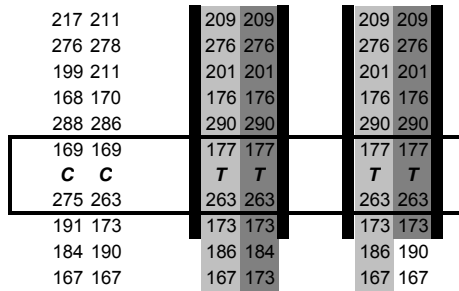
MARKERS	Mb	Band
centromere		
<i>D11S4143 (AFMb055yd1)</i> [#]	79.03	11q14.1
<i>VNTR19CA</i> [#]	79.28	
<i>D11S1362 (AFMa132xh9)</i> [#]	79.47	
<i>D11S901 (AFM063yg1)</i> [#]	81.52	
<i>D11S4187 (AFM311wh5)</i> [#]	83.23	
<i>D11S1354 (AFM338xe1)</i> [#]	84.35	
TMEM126A - c.163C	85.04	11q14.1
<i>D11S1887 (AFMa049wa5)</i> [#]	86.06	11q14.2
<i>D11S1780 (AFMa082wb9)</i> [#]	87.32	
<i>D11S1332 (AFM281wf9)</i> [#]	91.74	11q14.4
<i>VNTR29TA</i> [#]	93.41	11q21
telomere		



209	217
276	276
201	199
176	168
290	288
177	169
T	C
263	275
173	191
186	184
167	167

209	211
276	278
201	211
176	170
290	286
177	169
T	C
263	263
173	173
184	190
173	167

<i>D11S4143 (AFMb055yd1)</i> [#]	79.03	11q14.1
<i>VNTR19CA</i> [#]	79.28	
<i>D11S1362 (AFMa132xh9)</i> [#]	79.47	
<i>D11S901 (AFM063yg1)</i> [#]	81.52	
<i>D11S4187 (AFM311wh5)</i> [#]	83.23	
<i>D11S1354 (AFM338xe1)</i> [#]	84.35	
TMEM126A - c.163C	85.04	11q14.1
<i>D11S1887 (AFMa049wa5)</i> [#]	86.06	11q14.2
<i>D11S1780 (AFMa082wb9)</i> [#]	87.32	
<i>D11S1332 (AFM281wf9)</i> [#]	91.74	
<i>VNTR29TA</i> [#]	93.41	11q21



211	217
272	278
197	195
160	160
290	284
177	169
T	C
263	263
173	189
200	186
167	167

211	211
272	278
197	199
160	168
290	288
177	167
T	C
263	269
173	191
200	178
167	167

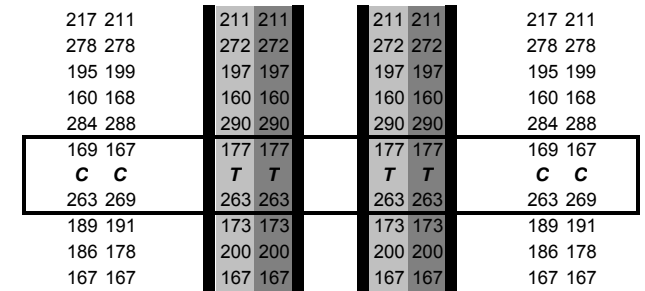
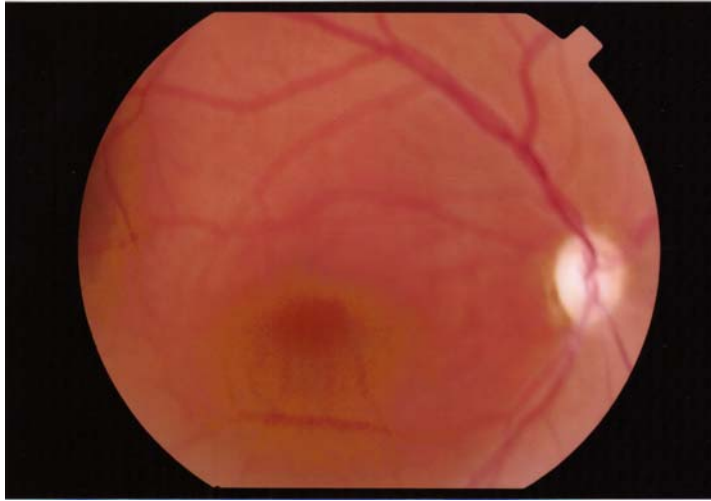


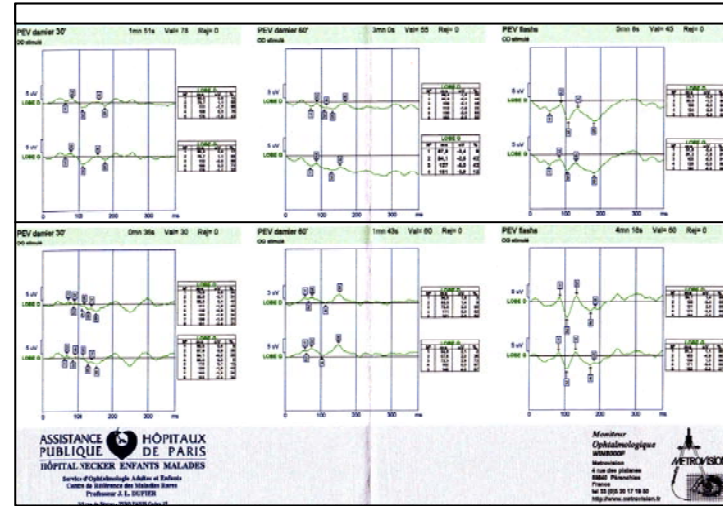
Figure S3. Ophthalmological data in 37-year-old patient III6, Family 1 harboring the *TMEM126* p.Arg55X mutation.

(A) The fundus photograph of left eye shows optic disc pallor with normal aspect of the retina including the macular region. (B) Flash visual evoked potentials (VEP) show flattened waves, prolonged latencies and highly reduced amplitudes for right eye (RE) and left eye (LE). Electroretinographic recordings were strictly normal. Pattern reversal VEP display hardly recordable traces. (C, D) Goldman Dynamic perimetry show severe bilateral visual field loss.

A



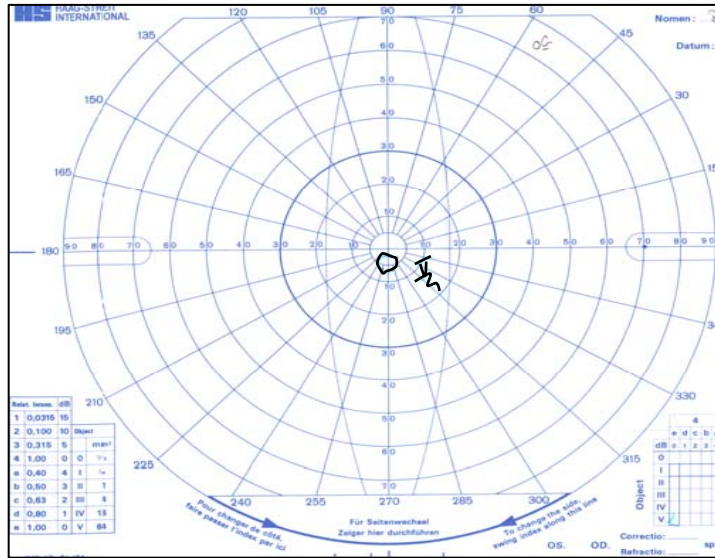
B



RE

LE

C



D

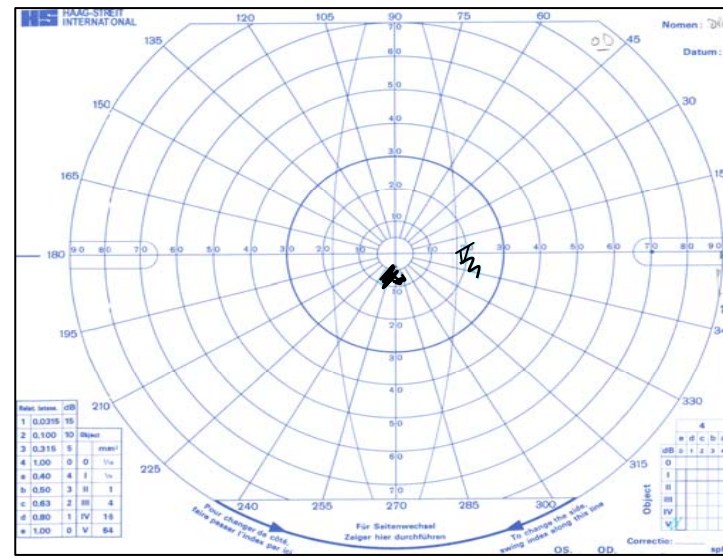


Figure S4. Brain Magnetic Resonance Imaging (MRI) of 37-year-old patient III6, Family 1 harboring the *TMEM126* p.Arg55X mutation.

(A) Axial FLAIR weighted images show asymmetric and homogeneous punctate hyperintensities with no evidence for necrosis (white arrows). (B) Coronal weighted FSE T2 and axial FLAIR images show hyperintensities in the bilateral stratum subependymale (left > right side) near the head and corpus of the caudate nuclei (black arrow).

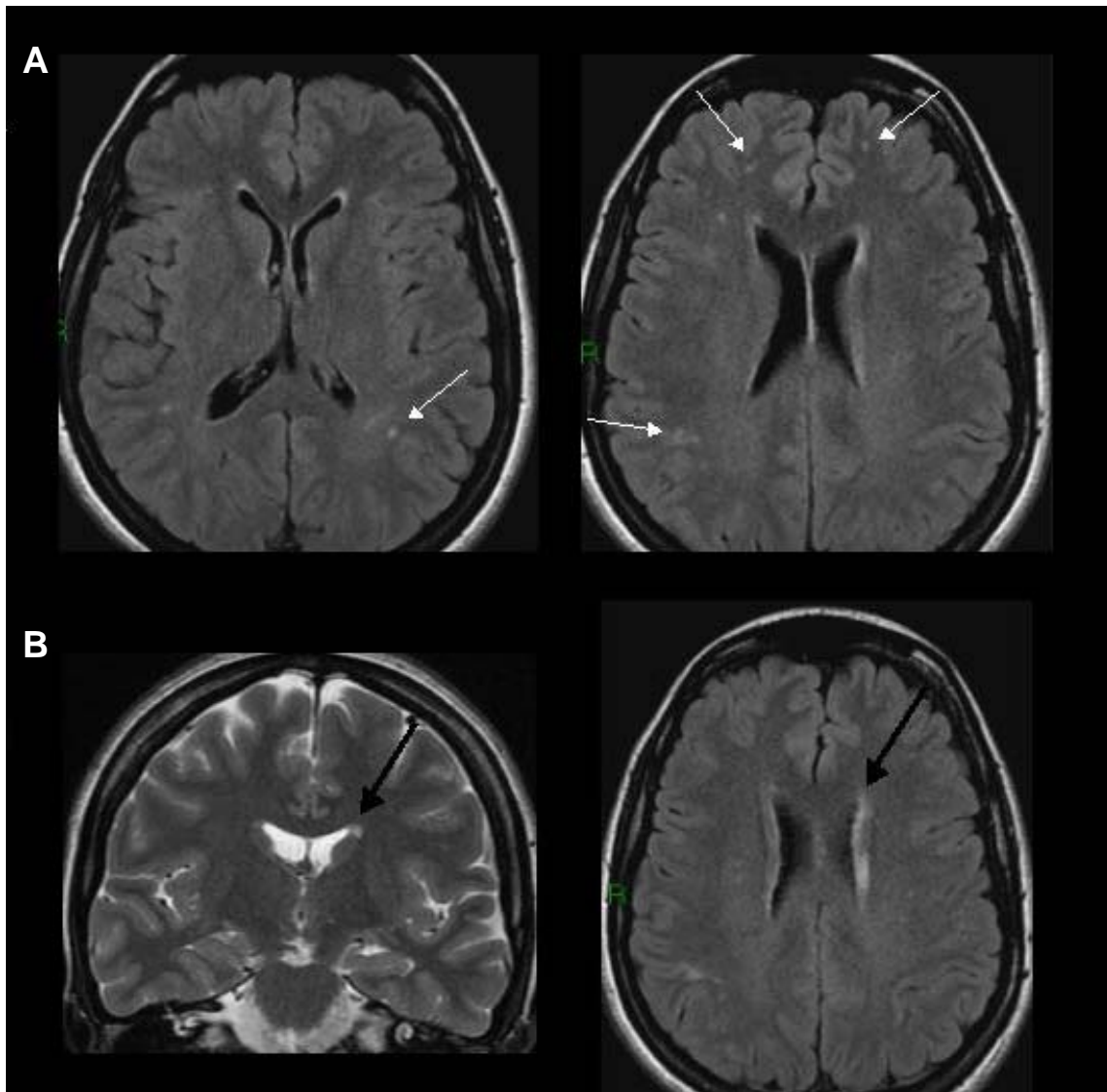


Figure S5. Expression of the TMEM126-myc fusion protein in COS-7 cells, 48 hours after transient transfection.

COS-7 cells were transfected with 1 µg plasmid DNA (OmicsLink ORF Expression Clone-GeneCopoeia™ clone EX-V0975-M09; Ressourcenzentrum fuer Genomforschung imaGenes) with FuGENE®6 transfection reagent, according to the manufacturer's instructions (Roche). The cells were fixed for 15 min in 4% formaldehyde, 48 hr post-transfection. Immunocytochemistry was performed via classical procedures. Colocalization experiments were performed using specific or myc antibodies (mouse monoclonal anti-myc and rabbit polyclonal anti-myc, 1/200, Santa Cruz Biotechnology), respectively. Secondary antibodies were Alexa Fluor®488 conjugated goat anti-rabbit (1/1000, Molecular Probes) and ZyMax™ goat anti-mouse CY™ 3 conjugate (1/100, Invitrogen). No significant colocalization of Transmembrane 126A protein was noted with Golgi apparatus (mouse monoclonal anti-Giantin, 1/200, Abcam), lysosomes (mouse monoclonal anti-Lamp2, 1/200, Abcam), endoplasmic-reticulum (mouse monoclonal anti-Calreticulin, 1/400, Stressgen), early endosomes (rabbit polyclonal anti-EEA1, 1/200, Abcam), cytoskeleton (mouse monoclonal anti-βActin, 1/100, AbCys) and microtubule (mouse monoclonal anti-γTubulin, 1/200, Sigma), respectively. Cells were counterstained and mounted with ProLong®Gold antifade reagent with DAPI (Invitrogen). Images were recorded using a Leica SP5 confocal microscope (objective 63x oil immersion objective, scale bar = 20 µm) and Leica Application Suite Advanced Fluorescence Lite software.

Expression of a myc-tagged fusion protein of the expected size was verified on Western blots of cell extracts with a myc antibody (mouse anti myc, 1/1000, Santa Cruz Biotechnology, data not shown).

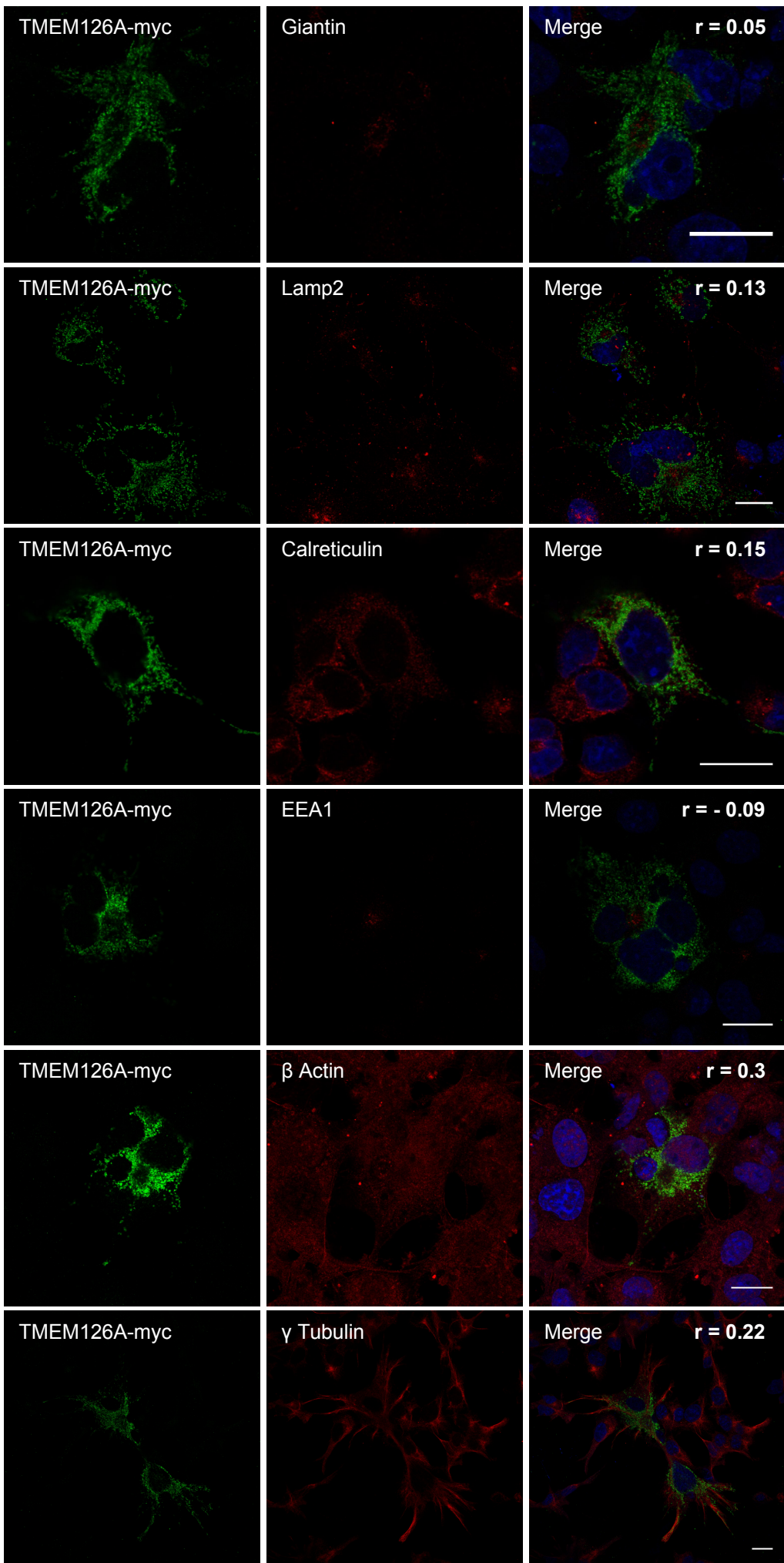
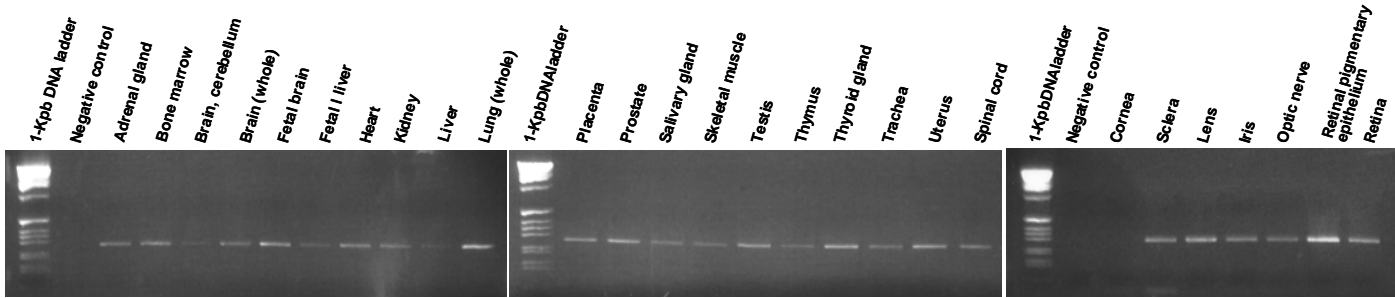


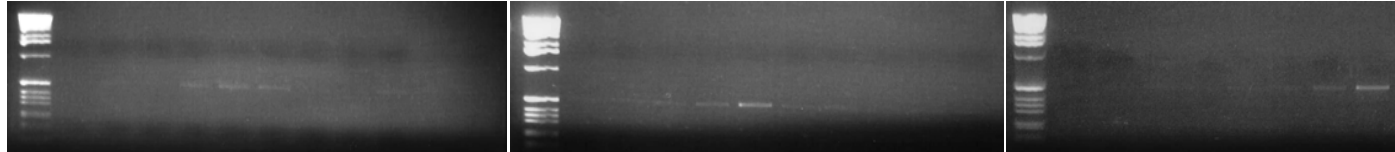
Figure S6. RT-PCR quantification of *TMEM126A* mRNA in human tissues.

TMEM126A mRNA expression was analyzed by RT-PCR in adult human tissues, normalized with respect to *vimentin* expression, (A) semi-quantitatively (at 25 PCR cycles, in the exponential phase) and (B) at end point PCR (et 35 cycles, in the plateau phase). One microgram of total RNAs from adrenal gland, bone marrow, brain (whole), cerebellum, fetal brain, fetal liver, lung (whole), placenta, prostate, salivary gland, skeletal muscle, testis, thymus, thyroid gland, trachea, uterus and spinal cord (Human Total RNA Master panel II, Clontech) were reverse transcribed with the High Capacity cDNA Archive Kit (Applied Biosystems) primed with Oligo d(T)16 (Applied Biosystems) in accordance with the supplier's recommendations. 0.5 microgram of total RNAs from retina, optic nerve, retinal pigmentary epithelium (RPE), cornea, iris, sclera and lens extracted from a twenty-week-old fetal human ocular globe were also reverse transcribed. A 523 pb cDNA fragment of *TMEM126A* from exon 2 to exon 5 was amplified using primer: (forward) 5'-taaccagcttcagaagcag-3', (reverse) 5'-gtgaattctttgccaggtca-3' (Genbank accession numbers NM_032273). A 274 bp cDNA fragment of *VIMENTIN* containing exons 1 to 4 was amplified using primers: (forward) 5'-accagctaaccaacgacaaa-3', (reverse) 5'-tgctgttctctgaatctgagc-3' (GenBank accession number NM_003380), as a reference. Semi-quantitative condition showed a predominantly expression in brain (whole), cerebellum, fetal brain, skeletal muscle, testis, fetal retinal pigmentary epithelium (RPE) and retina (A) while a widespread expression of *TMEM126A* mRNA in all adult tissues was noted (B).

A

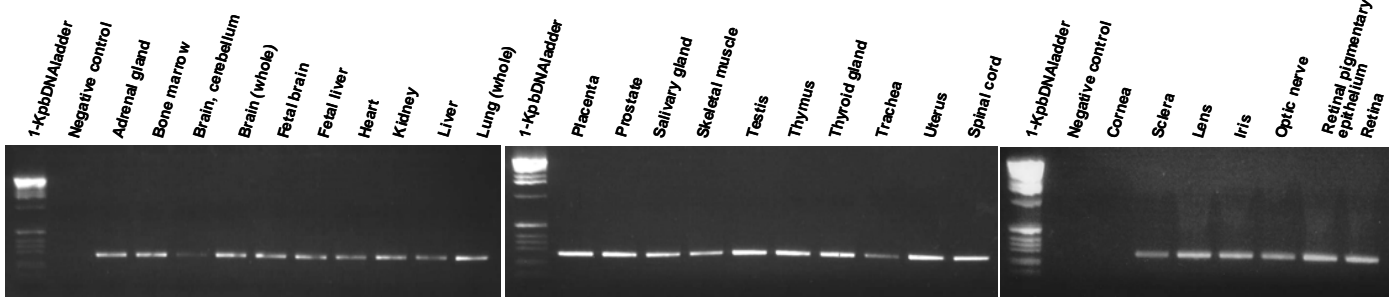


VIMENTIN, Exons 1-4

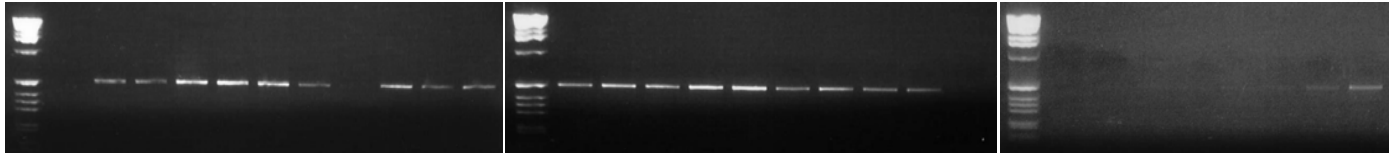


TMEM126A, Exons 2-4

B



VIMENTIN, Exons 1-4



TMEM126A, Exons 2-4

Table S1. Sequences of primers used for amplification of (A) four polymorphic markers developed from the UCSC Draft of the Human Sequence; and (B) the five exons of the *TMEM126* gene (Genbank accession number NM_032273).

A) Polymorphic markers (VNTR = variable number of tandem repeat).

VNTRs / chromosomal position	Forward sequence (5'-3')	Reverse sequence (5'-3')
VNTR19CA (79.28Mb)	tgccgggagcctaaat	actcacctgcagatcttag
VNTR23TG (79.67Mb)	gatacatgtatacattgtgt	gtaatcattttgacatgtt
VNTR29TA (93.41Mb)	tcactcaactcctgaacctc	aagatctaccccagtgeg
VNTR26AT (93.48Mb)	gcttctcattccctctctg	tagcctattgtgggaccc

B) *TMEM126*

Exon	Forward sequence (5'-3')	Reverse sequence (5'-3')
1	cttctcagcccaaagccgct	cgctcgtccttctcctgacac
2	cagattagctctacagtattat	ccttctcacattccatgttg
3	gggatagatgctgtatccag	attacagcatacagtacttgg
4	caattacattgatatattacctg	gggtaacattgcctttggtc
5	tttatcttaagacttctaggac	ccctttgttaggtcccag

Supplemental References

1. Abecasis, G.R., Cherny, S.S., Cookson, W.O., Cardon, L.R. (2002). Merlin-rapid analysis of dense genetic maps using sparse gene flow trees. *Nat. Genet.* 30, 97-101.